Journal of Reproduction and Development, Vol. 66, No 6, 2020

—Original Article—

Expression and functions of cluster of differentiation 9 and 81 in rat mammary epithelial cells

Kotaro HORIGUCHI[1)], Saishu YOSHIDA[2)], Takehiro TSUKADA[3)], Takashi NAKAKURA[4)], Ken FUJIWARA[5)], Rumi HASEGAWA[1)], Shu TAKIGAMI[1)] and Shunji OHSAKO[1)]

[1)]*Laboratory of Anatomy and Cell Biology, Department of Health Sciences, Kyorin University, Tokyo 181-8612, Japan*
[2)]*Department of Biochemistry, The Jikei University School of Medicine, Tokyo 105-8461, Japan*
[3)]*Department of Biomolecular Science, Faculty of Science, Toho University, Chiba 274-8510, Japan*
[4)]*Department of Anatomy, Graduate School of Medicine, Teikyo University, Tokyo 173-8605, Japan*
[5)]*Department of Biological Science, Kanagwa University, Kanagawa 259-1293, Japan*

Abstract. Cluster of differentiation (CD) 9 and CD81 are closely-related members of the tetraspanin family that consist of four-transmembrane domain proteins. *Cd9* and *Cd81* are highly expressed in breast cancer cells; however, their expression in healthy mammary glands is unclear. In this study, we performed quantitative real-time PCR to analyze the expression levels of *Cd9* and *Cd81*. Histological techniques were employed to identify *Cd9*- and *Cd81*-expressing cells in rat mammary glands during pregnancy and lactation. It was observed that *Cd9* and *Cd81* were expressed in the mammary glands, and their expression levels correlated with mammary gland development. To identify cells expressing *Cd9* and *Cd81* in the mammary glands, we performed double immunohistochemical staining for CD9 and CD81, prolactin receptor long form, estrogen receptor alpha, or Ki67. The results showed that CD9 and CD81 were co-expressed in proliferating mammary epithelial cells. Next, we attempted to isolate CD9-positive epithelial cells from the mammary gland using pluriBead cell-separation technology based on antibody-mediated binding of cells to beads of different sizes, followed by isolation using sieves with different mesh sizes. We successfully isolated CD9-positive epithelial cells with 96.8% purity. In addition, we observed that small-interfering RNAs against *Cd9* and *Cd81* inhibited estrogen-induced proliferation of CD9-positive mammary epithelial cells. Our current findings may provide novel insights into the proliferation of mammary epithelial cells during pregnancy and lactation as well as in pathological processes associated with breast cancer.
Key words: Cluster of differentiation (CD) 9, CD81, Lactation, Mammary gland, Proliferation

(**J. Reprod. Dev. 66:** 515–522, 2020)

Cluster of differentiation (CD) 9 (also known as TSPAN29, leukemia-associated cell surface antigen p24, and motility-related protein-1) is a member of the tetraspanin family that consists of four transmembrane domains, an intracellular terminus, and two extracellular loops [1]. CD9 participates in a variety of biological functions, including cell adhesion, migration, proliferation, metastasis, differentiation, and sperm–egg fusion [2]. CD9 was first described as a motility-related factor in a study that demonstrated that anti-CD9 antibody inhibited the migration and invasion of multiple cancerous cell lines [3, 4]. Data from numerous *in vitro* studies suggest that CD9 regulates the metastatic spread of tumor cells. Recently, CD9 has been recognized as a biomarker of invasion and late-stage breast cancer [5].

CD9 forms a complex with another member of the tetraspanin superfamily, CD81. It has been reported that adult *Cd9* and *Cd81* double-knockout (*Cd9/Cd81* DKO) mice exhibited pituitary atrophy and progressive weight loss owing to decreased bone mineral density, muscle mass, and visceral adipose tissue mass [6]. In addition, *Cd9/Cd81* DKO mice were also found to be infertile. Although *Cd9* and *Cd81* are expressed in breast cancer tissues [7], their expression levels and physiological functions in healthy mammary glands are unclear.

Mammary glands are specialized subcutaneous glands in mammals that aid in nourishing the offspring. Within the mammary glands, the main duct branches repeatedly to form numerous terminal ducts, forming multiple acini in the lobules. The mammary glands undergo significant variations in size during pregnancy and lactation, and their functional activity also changes. Under the influence of estrogen and progesterone produced by the corpus luteum and prolactin secreted by the anterior pituitary gland, the terminal duct epithelial cells proliferate to form secretory acini. After lactation, the number of acini decreases rapidly. However, the molecular basis of steroid-dependent epithelial cell proliferation during mammary gland development has not been studied. In the present study, we examined the involvement of CD9 and CD81 in this physiological process. We analyzed *Cd9* and *Cd81* expression in normal rat mammary glands during pregnancy and lactation, and examined their roles in mammary epithelial cell proliferation under the influence of diethylstilbestrol (DES).

Received: June 16, 2020
Accepted: August 4, 2020
Advanced Epub: August 21, 2020

Correspondence: K Horiguchi (e-mail: kota@ks.kyorin-u.ac.jp)

Materials and Methods

Animals

Adult Wistar rats were purchased from Japan SLC (Shizuoka, Japan). Eight- to ten-week-old female rats, weighing 180–220 g, were maintained in a 12-h light/dark cycle and provided *ad libitum* access to food and water. The rats were mated, and the day at which vaginal spermatozoa were first detected was designated as day 1 of pregnancy (P1), the day of parturition was designated as day 0 of lactation (L0), and the first day of weaning was designated as day 0 of weaning (W0). Vaginal smears were prepared daily and stained with methylene blue to determine the estrous stage of the rats. Female rats in metestrus stage were used in this experiment. The rats were sacrificed by exsanguination from the right atrium after being anesthetized with a combination of medetomidine (0.15 mg/kg; Zenyaku Kogyo, Tokyo, Japan), midazolam (2.0 mg/kg; Sandoz, Tokyo, Japan), and butorphanol (2.5 mg/kg; Meiji Seika Pharma, Tokyo, Japan). The rats were then perfused with Hanks' balanced salt solution (Thermo Fisher Scientific, Waltham, CA, USA) for isolation of CD9-positive cells from the mammary glands, or with 4% paraformaldehyde in 0.05 M phosphate buffer (pH 7.4) for *in situ* hybridization and immunohistochemistry. The current study was approved by the Committee on Animal Experiments of Kyorin University and followed the NIH Guidelines for the Care and Use of Laboratory Animals.

Quantification of mRNA levels using quantitative real-time polymerase chain reaction analysis

Quantitative real-time polymerase chain reaction (qPCR) was performed as described previously [8]. Total RNA was extracted from CD9-positive and CD9-negative mammary cells using RNeasy Plus Mini Kit (Qiagen, Hilden, Germany); contaminating DNA was removed by 15-min digestion at 22–23°C using RNase-free DNase Set (Qiagen). Next, cDNA was synthesized using ReverTra Ace qPCR RT Master Mix (Toyobo, Osaka, Japan). qPCR was performed in Thermal Cycler Dice Real Time System II (Takara Bio, Shiga, Japan) using gene-specific primers and SYBR Premix Ex Taq (Takara) containing SYBR Green I. The sequences of the gene-specific primers were as follows: *Cd9* (NM_053018), 5′-GGCTATACCCACAAGGACGA-3′ and 5′-GCTATGCCACAGCAGTTCAA-3′ (product length: 140 bp); *Cd81* (NM_013087), 5′-TCACTTGCCTTGTGATCCTG-3′ and 5′-GCATCATCATCCATCACAGC-3′ (product length: 136 bp); estrogen receptor alpha (*Esr1*) (NM_012689), 5′-ACCCATGGAACATTTCTGGA-3′ and 5′-GCTTTGGTGTGAAGGGTCAT-3′ (product length: 139 bp); prolactin receptor long form (*Prlrl*) (NM_001034111), 5′-CATCTGCACTTGCTTTCGTC-3′ and 5′-TCAGGAGAGCGACATTTGTG-3′ (product length: 100 bp); platelet and endothelial cell adhesion molecule 1 (*Pecam1*) (NM_031591), 5′-TCTGCTGCCGTCAAATACTG-3′ and 5′-GACCAGGCAAACCTGAGAAG-3′ (product length: 117 bp); β-casein (*Csn2*) (NM_017120), 5′-CACAAACAGATGCCCTTCCT-3′ and 5′-GTCTGAGGAAAAGCCTGCAC-3′ (product length: 143 bp); and hypoxanthine phosphoribosyltransferase 1 (*Hprt1*) (NM_012583), 5′-CTCATGGACTGATTATGGACAGGAC-3′ and 5′-GCAGGTCAGCAAAGAACTTATAGCC-3′ (product length: 123 bp). *Hprt1* served as the reference gene for normalization of gene expression [9]. Relative gene expression levels were calculated by comparing the cycle threshold (Ct) value of each target with that of the reference gene. Ct values were converted to relative gene expression levels using the formula $2^{-(\Delta Ct\ sample\ -\ \Delta Ct\ control)}$. The expression level of each target mRNA was analyzed in at least three independent experiments.

Tissue preparation

Mammary glands obtained from female rats were immediately immersed in 4% paraformaldehyde in 0.05 M phosphate buffer (pH 7.4) and incubated for 20–24 h at 4°C. Next, the tissues were immersed in phosphate buffer (pH 7.2) containing 30% sucrose, incubated for more than 2 days at 4°C, embedded in Tissue-Tek O.C.T. compound (Sakura Finetek Japan, Tokyo, Japan), and frozen rapidly. The frozen tissues were sectioned (8-μm thick) using a cryostat (Tissue-Tek Polar DM; Sakura Finetek Japan) and mounted on glass slides (Matsunami, Osaka, Japan).

In situ hybridization and immunohistochemistry

In situ hybridization was performed with digoxigenin (DIG)-labeled complementary RNA (cRNA) probes, as described in our previous report [10]. A fragment of the *Cd9* gene was PCR-amplified from rat pituitary cDNA library using the following primer pair: 5′-GGCTATACCCACAAGGACGA-3′ and 5′-CCCGGATCCCTCTACTACAA-3′ (product length: 528 bp). The amplified cDNA was ligated into the pTA-2 vector (Toyobo) and subcloned into a plasmid vector. Gene-specific antisense and sense DIG-labeled cRNA probes were generated using Roche DIG RNA Labeling Kit (Roche Diagnostics, Basel, Switzerland). Visualization of each type of mRNA was performed using alkaline phosphatase-conjugated anti-DIG antibodies (Roche Diagnostics) and the substrates 4-nitroblue tetrazolium chloride and 5-bromo-4-chloro-3-indolyl phosphate (BCIP; Roche Diagnostics). All observations were performed in triplicate.

For fluorescent double labeling of *Cd9* mRNA, *in situ*-hybridization signals were visualized using HNPP Fluorescent Detection Kit (Roche Diagnostics). After *in situ* hybridization, the sections or cells were incubated for 20 min at 30°C in phosphate-buffered saline (PBS; pH 7.2) containing 2% normal donkey serum, followed by incubation at 22–23°C with different primary antibodies (Table 1). Next, the cells were washed with PBS and incubated with PBS containing secondary antibodies for 30 min at 30°C (Table 1). The absence of detectable nonspecific reactions was confirmed using normal mouse and rabbit sera. Nuclei were counterstained by incubation with Vectashield mounting medium containing 4,6-diamidino-2-phenylindole (DAPI; Vector Laboratories, Burlingame, CA, USA), and the sections were scanned using a fluorescence microscope (cellSens Dimension System; Olympus, Tokyo, Japan). All observations were performed in triplicate.

For double immunofluorescence, frozen sections or cells were incubated overnight at 22–23°C in PBS containing anti-CD9 antibody together with anti-CD81 [11], anti-estrogen receptor α (anti-ERα) [12], anti-prolactin receptor (anti-PRLR) [13], or anti-CD133 (a stem/progenitor cell marker) [14] antibody. The primary and secondary antibodies used in this study are listed in Table 1. Next, the cells

Table 1. Primary and secondary antibodies used for immunohistochemistry and immunocytochemistry

Primary antibody target	Type	Dilution	Source; Catalog number
CD9	Mouse monoclonal	1:100	BD Pharmingen; 551808
CD81	Hamster monoclonal	1:800	Acris; SM1526PS
Ki67	Mouse monoclonal	1:100	DAKO; M7240
PRLR	Rabbit monoclonal	1:100	Abcam; ab170935
CD133	Rabbit polyclonal	1:100	Novus Biologicals; NB120-16518SS
ERα	Rabbit polyclonal	1:100	Santa cruz; sc-542
BrdU	Rabbit polyclonal	1:100	Rockland INC.; 600-401-C29S
Secondary antibody		Dilution	Source; Catalog number
Alexa Fluor 568-conjugated donkey anti-mouse IgG		1:100	Thermo Fisher Scientific; A-10037
Alexa Fluor 488-conjugated donkey anti-rabbit IgG		1:100	Thermo Fisher Scientific; A-11055
Alexa Fluor 488-conjugated goat anti-hamster IgG		1:100	Thermo Fisher Scientific; A-21110

were washed with PBS and incubated in PBS containing secondary antibodies, as described above. Sections and cells were scanned using a fluorescence microscope (cellSens Dimension System; Olympus). All observations were performed in triplicate.

To calculate the proportion of immunopositive cells, three different areas (157.5 × 210 μm^2) per experimental group were selected, and the number of immunopositive cells was counted using cellSens Dimension system (Olympus).

Isolation of CD9-positive cells from mammary glands

At L30, the mammary glands of female rats were excised, minced into small pieces, and incubated in Medium 199 with Earle's salts (Thermo Fisher Scientific) containing 0.2% collagenase (Wako Pure Chemicals, Osaka, Japan) for 60 min at 37°C. Next, the minced pieces of mammary glands were incubated with 1% trypsin (Thermo Fisher Scientific) and 0.2% collagenase containing 5 μg/mL DNase I (Thermo Fisher Scientific) for 10 min at 37°C, followed by incubation in Hanks' solution containing 0.3% ethylenediaminetetraacetic acid (Wako Pure Chemicals) for 5 min at 37°C and washing with Medium 199. Dispersed cells were separated from debris by centrifugation, rinsed, resuspended in Medium 199 by pipetting, and filtered through nylon mesh (Becton Dickinson Labware, Franklin Lakes, NJ, USA). The dispersed cells were separated using the pluriBead-cascade Cell Isolation System (Universal Mouse pluriBeads kit; pluriSelect Life Science, Leipzig, Germany), as described previously [10], with mouse monoclonal anti-CD9 antibodies (BD Biosciences, Franklin Lakes, NJ, USA), according to the manufacturer's instructions. Subsequently, CD9-positive and CD9-negative cells were counted and subjected to qPCR analysis or plated on glass slides for smear preparation or cultivation. CD9-positive cells were plated on 8-well glass chamber slides (1 cm^2/well; Thermo Fisher Scientific) coated with laminin (10 μg/cm^2; Merck Millipore, Darmstadt, Germany) at a density of 1×10^5 cells/cm^2 in 400 μl of Medium 199 (without phenol red) supplemented with 10% charcoal/dextran-treated fetal bovine serum (FBS; Sigma-Aldrich, St. Louis, MO, USA), 0.5 U/ml of penicillin, and 0.5 μg/ml of streptomycin (Thermo Fisher Scientific). The cells were then cultured for 72 h at 37°C in a humidified atmosphere of 5% CO_2 and 95% air.

Quantification of CD9-positive cells

Five random fields were imaged per slide for smear preparation of isolated CD9-positive cell fraction using a fluorescence microscope with a 40-fold objective lens. The number of CD9-positive cells and the total number of DAPI-stained cells per unit area (157.5 × 210 μm^2) were counted using cellSens Dimension System (Olympus). Observations were performed in triplicate for each experimental group.

Small interfering RNA-mediated knockdown

CD9-positive cells isolated from rat mammary glands were plated at a density of 1.0×10^5 cells/cm^2 on 8-well glass chamber slides coated with laminin. The cells were then cultured at 37°C for 24 h in 400 μl of Medium 199 containing 10% FBS (Merck Millipore) in a humidified atmosphere of 5% CO_2 and 95% air. For small interfering RNA (siRNA) transfection, the culture medium was replaced with 400 μl of Medium 199 containing 10% FBS (Thermo Fisher Scientific) supplemented with the transfection reagent INTERFERin (1:100 v/v; PolyPlus Transfection, Illkirch, France) and siRNAs against *Cd9* or/and *Cd81* (0.2 μM Mm_*Cd9*_1 and Mm_*Cd81*_2; Qiagen), and the cells were incubated for 48 h. An siRNA without homology to any known mammalian gene was used as the negative control (SI03650325; Qiagen). The cultivated cells were used for proliferation assays and immunocytochemistry.

Cell proliferation assay

To visualize cell proliferation, primary cell cultures were incubated with the nucleotide analog 5-bromo-2′-deoxyuridine (BrdU, 3 μg/ml; Sigma-Aldrich) and a synthetic estrogen analogue (DES, 1×10^{-8} M; Merck Millipore) for 24 h. The cells were fixed in 4% paraformaldehyde in 25 mM phosphate buffer (pH 7.4) for 20 min at 20–23°C, and then treated with 4 N HCl in PBS for 10 min. Next, the cells were incubated in PBS containing 2% normal donkey serum for 30 min at 30°C, followed by overnight incubation with rabbit anti-rat BrdU polyclonal antibody and mouse monoclonal anti-CD9 antibody at 22–23°C (Table 1). The cells were then washed with PBS and incubated with PBS containing appropriate secondary antibodies (Table 1). Five random fields per well were imaged using a fluorescence microscope with a 40-fold objective lens. Observations were performed in triplicate for each experimental group.

Statistical analysis

Data are presented as mean ± SEM of at least three independent experiments for each group of rats. F tests and subsequent Student's *t*-tests were used for two-group comparisons. Significant differences between control and experimental groups were determined by performing Dunnett's test. The results are indicated together with P-values.

Results

Identification of CD9-positive cells in rat mammary glands

qPCR was used to determine *Cd9* expression in female mammary cells during metestrus, pregnancy, lactation, and weaning. We also quantified the expression levels of *Cd9*, *Cd81*, *Prlrl*, and *Csn2* in female rats, and found that the expression levels of these genes were higher during pregnancy and lactation than those during metestrus (Fig. 1). Figure 2A shows hematoxylin and eosin staining of mammary gland cryosections from female rats at postnatal day 60. *Cd9* mRNA was detected in the mammary glands of female rats using *in situ* hybridization with DIG-labeled antisense cRNA probe (Fig. 2B). Cells expressing *Cd9* mRNA were located in the acinus and duct cells of the mammary glands. No specific signal was detected in sections processed with DIG-labeled sense *Cd9* RNA probe (data not shown). We performed double-staining using *in situ* hybridisation for *Cd9* and immunohistochemistry for CD9. CD9-positive cells expressed *Cd9* (Fig. 2C), indicating that this immunoreactivity did not represent non-specific staining. Immunoreactive CD9 signals were located on the membranes of mammary cells (Fig. 2D). To identify the cell types expressing CD9, we double-stained the mammary gland at L10 with anti-CD9 antibody and anti-CD81, anti-ERα, anti-PRLR, or anti-CD133 antibody. The results indicated that CD81 and CD133 were located on the cell membrane, while ERα was localized in the nucleus of mammary epithelial cells (Fig. 3A). PRLR was detected in the cell membrane as well as in the cytoplasm (Fig. 3A). CD9 was co-localized with CD81, and was detected in cells expressing *Esr1*, *Prlrl*, and *Cd133*, suggesting that *Cd9* and *Cd81* were expressed in mammary epithelial cells (Fig. 3, white line arrowheads). In addition, Ki67-specific signals were detected in the nucleus of *Cd9*-expressing cells by *in situ* hybridization (Fig. 3A). We also detected CD9-negative cells that expressed *Cd81*, *Cd133*, or *Esr1* in the mammary gland (Fig. 3A, white arrowheads). The proportions of CD81-, ERα-, PRLR-, CD133-, and Ki67-positive cells among CD9-positive cells were 99.0 ± 0.4, 23.4 ± 25, 89.4 ± 3.4, 48.3 ± 4.3, and 4.3 ± 0.6%, respectively (Fig. 3B). Thus, the number of ERα- and Ki67-positive cells in the mammary gland were low. On the other hand, the proportion of CD9-positive cells among CD81-, ERα-, PRLR-, CD133-, or Ki67-positive cells was 99.1 ± 0.2, 97.4 ± 1.1, 95.6 ± 2.2, 98.0 ± 1.3, and 99.4 ± 0.6%, respectively (Fig. 3B). These data indicate that most of the CD81-, ERα-, PRLR-, CD133-, and Ki67-positive cells were CD9-positive.

Isolation of CD9-positive cells from the mammary glands

We attempted to purify CD9-positive cells using the pluriBead-cascade Cell Isolation System with monoclonal anti-rat CD9 antibody. One drop of the CD9-positive cell fraction recovered using this system was used for smear preparation and immunocytochemistry. In the recovered fraction, 96.8 ± 0.9% of the cells were CD9-positive (Fig. 4A). After primary culture of CD9-positive cells, the cells became double positive for CD9 and CD81 (Fig. 4B). qPCR showed that *Cd9* and *Cd81* mRNA levels in the CD9-positive cell fraction were increased by more than 5-fold as compared to those in the CD9-negative cell fraction (Fig. 4C). *Prlrl* and *Esr1* were also expressed by mammary epithelial cells, and their mRNA levels were higher in the CD9-positive cell fraction than those in the CD9-negative cell fraction (Fig. 4C). Conversely, the mRNA level of *Pecam1* (an endothelial cell marker) was significantly lower (P < 0.01) in the CD9-positive cell fraction than that in the CD9-negative cell fraction (Fig. 4C). These data indicate that the CD9-positive cells were mammary epithelial cells and that the purification was successful.

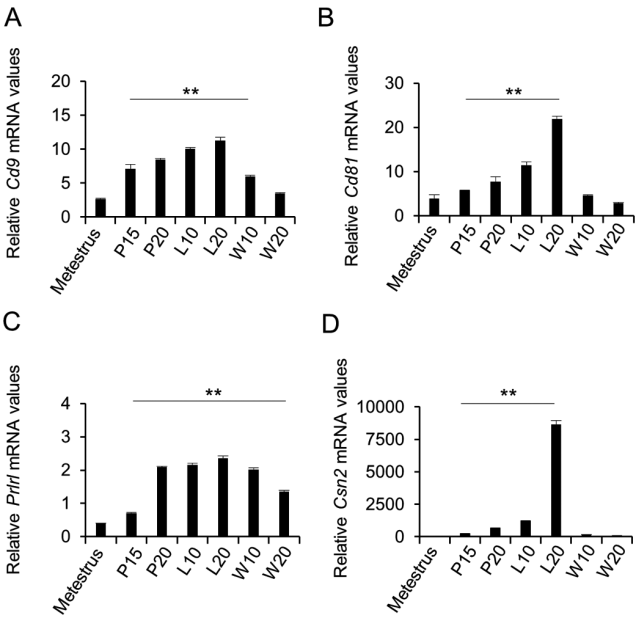

Fig. 1. Expression of *Cd9* and *Cd81* in the mammary glands of female rats during pregnancy and lactation. (A) *Cd9*, (B) *Cd81*, (C) prolactin receptor long form (*Prlrl*), and (D) β-casein (*Csn2)* mRNA expression levels in the mammary glands at metestrus, pregnancy day 15 (P15), P20, lactation day 10 (L10), L20, weaning day 10 (W10), and W20 were determined using real-time PCR (mean ± SEM, n = 3), followed by normalization to the expression of an internal control (*Hprt1*). ** $P < 0.01$.

Roles of CD9 and CD81 in mammary epithelial cell proliferation

CD9 and CD81 can associate with various integrins [15, 16]. Previously, we found that the proliferation of CD9-positive cells in the pituitary gland was markedly increased by laminin, an extracellular matrix component of the basement membrane [10]. Furthermore, it has been reported that the proliferation of mammary epithelial cells is enhanced by estrogen treatment [17, 18]. To examine the functional roles of CD9 and CD81, we knocked down *Cd9* or/and *Cd81* gene expression using siRNAs in purified CD9-positive cells cultured on laminin-coated surfaces. The expression levels of *Cd9* and *Cd81* were successfully downregulated by treatment with *Cd9*- and *Cd81*-siRNAs, respectively (Fig. 5A and B). Similar on-target results

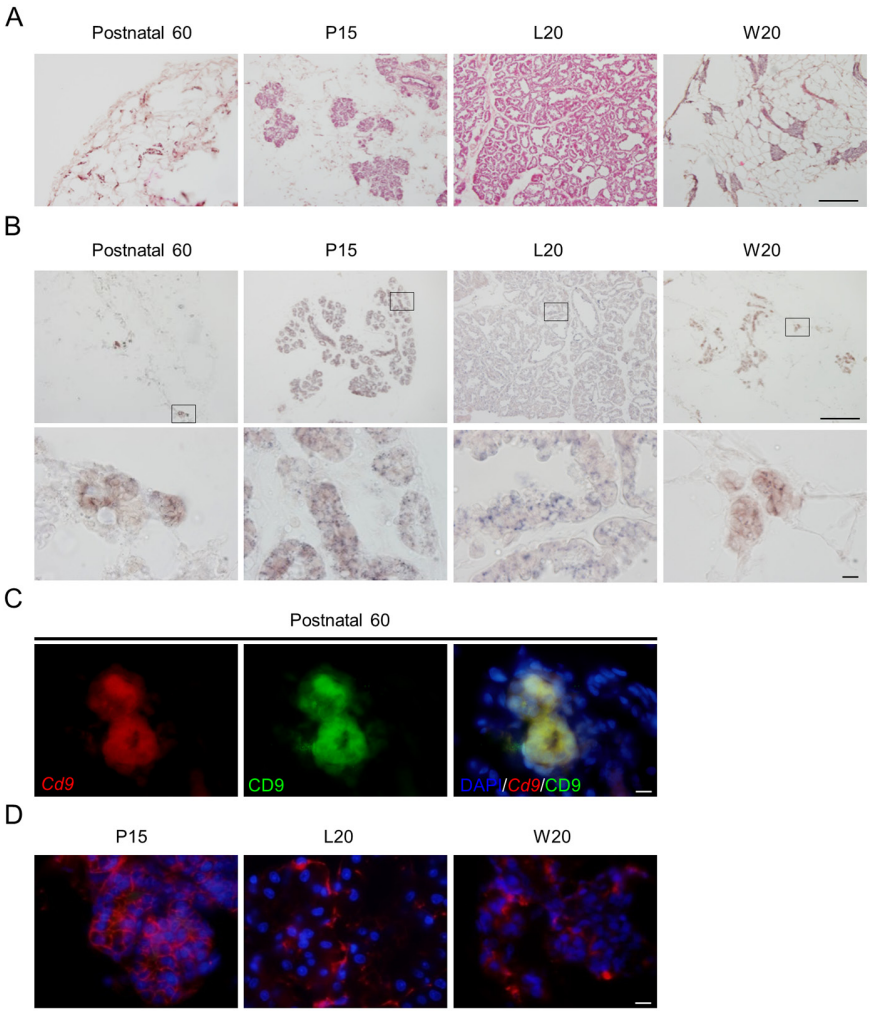

Fig. 2. Immunohistochemistry of CD9-positive cells in the mammary glands during pregnancy and lactation. (A) Hematoxylin and eosin staining of a cryosection of female rat mammary gland at postnatal day 60 (Postnatal 60), pregnancy day 15 (P15), lactation day 20 (L20), and weaning day 20 (W20). (B) *In situ* hybridization of *Cd9* at Postnatal 60, P15, L20, and W20 (upper panels). High-magnification images (lower panels) correspond to the boxed regions shown in the upper panels. (C) *In situ* hybridization of *Cd9* (red, left panel) and immunohistochemistry of CD9 (green, middle panel) at Postnatal 60. Merged images of them and DAPI staining (right panel). (D) Merged images of DAPI staining (blue) and immunofluorescence staining for CD9 (red) at P15, L20, or W20. Scale bars: 100 μm (upper panels of A and B) or 10 μm (lower panel of B; panels of C and D).

were obtained when the cells were co-transfected with *Cd9*- and *Cd81*-siRNAs (Fig. 5A and B), although *Cd81* expression increased following treatment with *Cd9*-siRNA (Fig. 5B). The expression levels of *Prlrl* and *Csn2* were not significantly altered by transfection with *Cd9*- or *Cd81*-siRNA (Fig. 5C and D).

Next, we examined the effect of DES (an estrogen analog) on *Cd9* and *Cd81* gene expression in purified CD9-positive cells cultured on laminin-coated surfaces. It was observed that DES treatment increased the expression levels of *Cd9*, *Cd81*, *Prlrl*, and *Csn2* (Fig. 6A and B). The expression levels of *Cd9* and *Cd81* were successfully downregulated by treatment with *Cd9*- and *Cd81*-siRNAs, respectively (Fig. 6). *Cd9*, *Cd81*, *Prlrl*, and *Csn2* expression levels were not upregulated by DES treatment in the siRNA-treated cells (Fig. 6). Moreover, after DES treatment, the proportion of BrdU-positive cells in the CD9-positive cell fraction co-transfected with *Cd9*- and *Cd81*-siRNA was significantly lower than that in the CD9-positive cell fraction transfected with non-silencing siRNA (Fig. 7A). Similarly, the number of BrdU-positive cells in the CD9-positive cell fraction transfected with *Cd9*- or *Cd81*-siRNA was clearly lower than that in the CD9-positive cell fraction transfected with non-silencing siRNA under the influence of DES (data not shown). Consistently, the percentage of BrdU-positive cells among CD9-positive cells co-transfected with *Cd9*- and *Cd81*-siRNA was 1.6 ± 1.2%, and the percentage of BrdU-positive cells among CD9-positive cells transfected with non-silencing siRNA was 9.4 ± 0.6% (Fig. 7B).

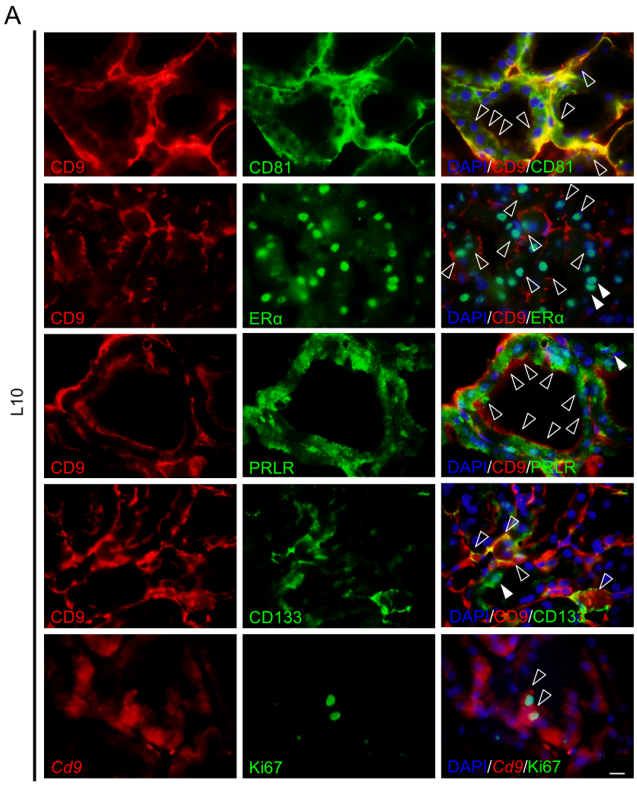

B

	Proportion (%)
CD81+ cells/CD9+ cells	99.0 ± 0.4
CD9+ cells/CD81+ cells	99.1 ± 0.2
ERα+ cells/CD9+ cells	23.4 ± 2.5
CD9+ cells/ERα+ cells	97.4 ± 1.1
PRLR+ cells/CD9+ cells	89.4 ± 3.4
CD9+ cells/PRLR+ cells	95.6 ± 2.2
CD133+ cells/CD9+ cells	48.3 ± 4.3
CD9+ cells/CD133+ cells	98.0 ± 1.3
Ki67+ cells/*Cd9*+ cells	4.3 ± 0.6
Cd9+ cells/Ki67+ cells	99.4 ± 0.6

Fig. 3. Characterization of CD9-positive cells in the mammary glands at L10. (A) Double immunofluorescence staining of CD9 (left panels) and CD81, ERα, PRLR, or CD133 (top 4 middle panels). *In situ* hybridization of *Cd9* (left panel) and immunofluorescence staining of Ki67 (bottom middle panel). The right panels show merged images of the left and middle panels, together with DAPI staining. Scale bar, 10 μm. White line arrowheads indicate double-positive cells. White arrows indicate CD9-negative cells. (B) Population of CD9-positive (CD9+) cells and cells positive for CD81 (CD81+), ERα (ERα+), PRLR (PRLR+), and CD133 (CD133+), or *Cd9*-expressing (*Cd9*+) cells and Ki67-positive (Ki67+) cells in the mammary gland at L10.

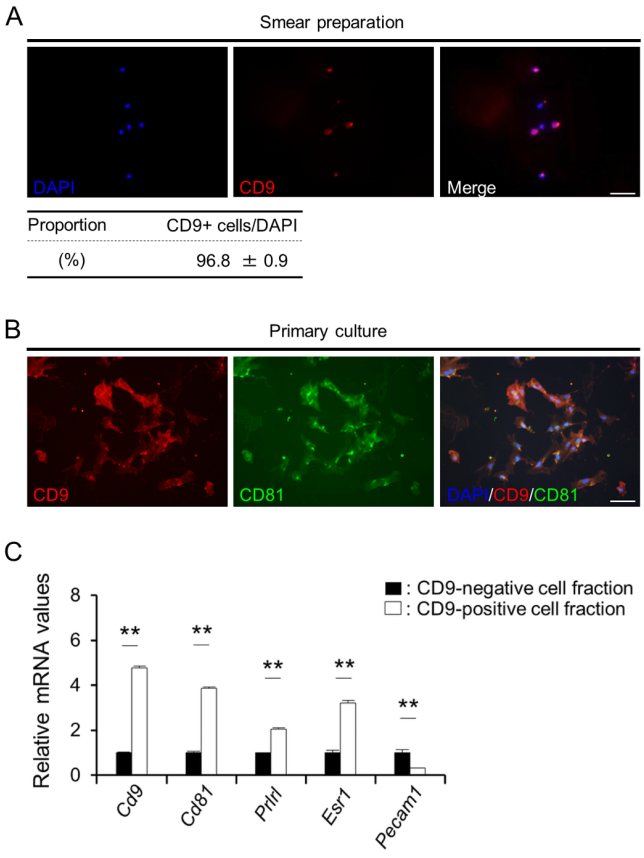

Fig. 4. Isolation of CD9-positive cells from female rat mammary glands at L30. (A) DAPI staining (blue) and immunofluorescence staining of CD9 (red) in a smear of CD9-positive cell fraction. The proportion of CD9-positive (CD9+) cells in the CD9-positive cell fraction obtained using pluriBeads are indicated (mean ± SEM, n = 3). The numbers of DAPI-positive and immunopositive cells were counted in random areas of the smear, and the proportion of CD9-positive cells was calculated. (B) Immunofluorescence staining of CD9 in the CD9-positive cell fraction cultured for 72 h. (C) The ratio of the mRNA expression levels of *Cd9*, *Cd81*, *Esr1*, *Prlrl*, and *Pecam1* in CD9-positive cells (white bars) against those in CD9-negative cells (*black bars*) was determined using qPCR (mean ± SEM, n = 6), followed by normalization to an internal control (*Hprt1*). The graph shows the relative expression levels of *Cd9*, *Cd81*, *Prlrl*, *Esr1*, and *Pecam1*. ** $P < 0.01$. Scale bars, 50 μm.

Discussion

The mammary gland undergoes significant variations in size and functional activity during pregnancy, lactation, and weaning. In pregnancy and lactation, elevated levels of circulating estrogen induces rapid growth in the length and branching of mammary ducts. The present study revealed that *Cd9* and *Cd81* were expressed in the epithelial cells of rat mammary glands. Using purified CD9-positive mammary epithelial cells, we demonstrated that CD9 and CD81 were associated with estrogen-mediated cell proliferation. Thus, CD9 and CD81 in the mammary epithelial cells are suggested to play key roles in the rapid growth of mammary gland during pregnancy and lactation.

CD9 is a member of the tetraspanin superfamily that forms a complex with CD81. The expression of *Cd9* gradually increased

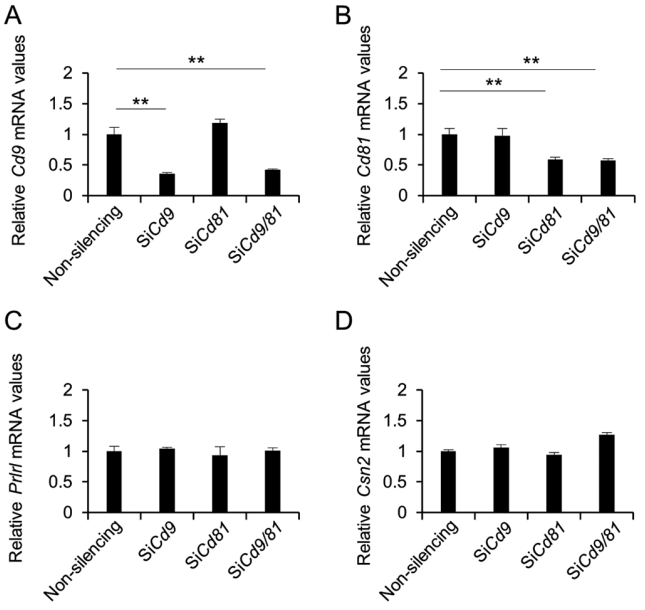

Fig. 5. Downregulation of *Cd9*, *Cd81*, *Prlrl*, and *Csn2* mRNA levels after transfection of CD9-positive mammary epithelial cells with the indicated siRNAs. (A) *Cd9*, (B) *Cd81*, (C) *Prlrl*, and (D) *Csn2* mRNA levels in CD9-positive cells transfected with non-silencing siRNAs, *Cd9*-siRNA, *Cd81*-siRNA, or *Cd9*-siRNA plus *Cd81*-siRNA for 48 h, as determined using qPCR (mean ± SEM, n = 3), followed by normalization to an internal control (*Hprt1*). ** $P < 0.01$.

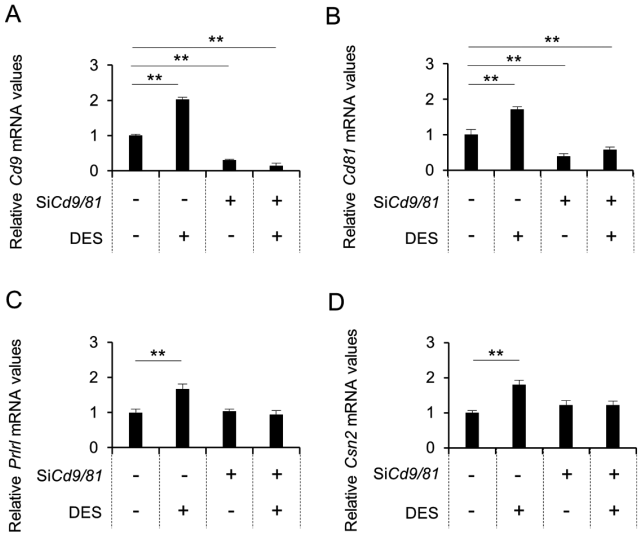

Fig. 6. Downregulation of *Cd9* and *Cd81* mRNA levels after transfection of CD9-positive mammary cells with siRNAs and DES treatment. (A) *Cd9*, (B) *Cd81*, (C) *Prlrl*, and (D) *Csn2* mRNA expression levels in CD9-positive cells cultured with non-silencing siRNAs or *Cd9*- and *Cd81*-siRNAs (black bars) for 48 h, with or without DES, as determined using qPCR (mean ± SEM, n = 3), followed by normalization to an internal control (*Hprt1*). ** $P < 0.01$.

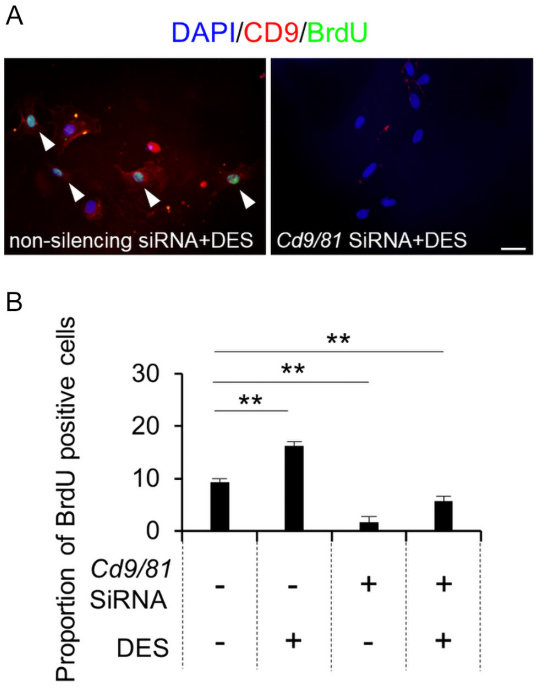

Fig. 7. The number of BrdU-positive cells among purified CD9-positive cells treated with DES. (A) Merged images showing DAPI staining (blue), BrdU immunocytochemistry (green), and CD9 immunocytochemistry (red) 48 h after CD9-positive cells were cultured with non-silencing siRNAs (left) or *Cd9*- and *Cd81*-siRNAs (right), with or without DES (as indicated). Arrowheads indicate cells that were double-positive for CD9 and BrdU. Scale bar, 10 μm. (B) Proportion of BrdU-positive cells among CD9-positive cells (mean ± SEM, n = 3). ** $P < 0.01$.

during pregnancy and lactation, and decreased during weaning. The expression pattern of *Cd9* was similar to that of *Prlrl* but not to those of *Csn2* and *Cd81*. We elucidated the effect of estrogen on the expression of *Cd9* and *Prlrl*, and found that DES treatment increased the expression of *Cd9* and *Prlrl* and consequently the number of CD9-positive mammary cells. These results suggest that the expression of *Cd9* and *Prlrl* during pregnancy and lactation is influenced by estrogen. Although estrogen increased the expression of *Csn2* and *Cd81* also, their expression was transient during lactation. It is well known that the site and phase of actions of estrogen and prolactin in the mammary gland are different. For instance, estrogen is essential for elongation and expansion of the ducts into mammary fat pad and lateral branching in the mammary gland during pregnancy; on the other hand, prolactin is mainly involved in alveolar development in the mammary gland, and it acts in a tightly-regulated hormonal milieu to promote lobulo-alveolar development and increase the expression of milk components during lactation [19–22]. Thus, it is suggested that transient increases in the expression of *Csn2* and *Cd81* during lactation may be enhanced by prolactin as well as estrogen, and that *Cd81* may contribute to alveolar development.

CD9 and CD81 interact with integrins, and the migratory, invasive, and proliferative functions of CD9 are attributed to its modulatory activity towards integrin complexes [23, 24]. *In vivo*, mammary epithelial cells interact with the basement membrane *via* integrins [25]. An important role of integrin in the mammary glands during pregnancy and lactation is lobulo-alveolar development, which

requires regulation of mammary cell proliferation and survival [26]. In the present study, downregulation of both *Cd9* and *Cd81* inhibited the proliferation of CD9-positive epithelial cells in the presence of laminin. These results suggest that CD9 and CD81 complexes sustain the proliferation of mammary epithelial cells *via* integrin signaling. The mammary gland undergoes striking changes in terms of size and cell numbers during puberty, pregnancy, lactation, and weaning. Upregulation of *Cd9* and *Cd81* may trigger the proliferation of CD9-positive mammary epithelial cells. Therefore, inhibition of CD9 and CD81 can serve as a potential strategy for preventing breast cancer cell proliferation *in vivo*.

It is well known that CD9 can suppress or promote breast cancer metastasis [27]. Data from recent studies have revealed that cells secrete exosomes, a novel type of extracellular vesicle with a lipid bilayer, that aid cancer metastasis [28]. CD9 and CD81 are now recognized as specific exosomal markers [28, 29]. The abundance of exosomes increases in comparison with mammary epithelial cells during pregnancy and lactation [30], which is in agreement with the results of the present study. Exosomes function as long-range messenger particles that mediate cell–cell communication. Our results suggest that CD9 and CD81 play important roles in mammary cell proliferation. However, their roles in exosome are currently unclear; and we plan to conduct relevant experiments in the future.

In conclusion, our data reveal that CD9 and CD81 were expressed in mammary epithelial cells, and downregulating their expression inhibited cell proliferation. In addition, we succeeded in isolating CD9-positive mammary epithelial cells with 96.8% purity utilizing anti-CD9 antibodies and pluriBead-cascade cell isolation system. These findings improve our understanding of the changes that mammary gland undergo during pregnancy and lactation.

Acknowledgements

We are grateful to Dr T Kato and Y Kato (Institute for Reproduction and Endocrinology, Meiji University) for their helpful discussions. This work was supported by JSPS KAKENHI Grants (nos. 16K08475 and 19K 07255) to KH.

References

1. **Berditchevski F, Odintsova E.** Tetraspanins as regulators of protein trafficking. *Traffic* 2007; **8**: 89–96. [Medline] [CrossRef]
2. **Brosseau C, Colas L, Magnan A, Brouard S.** CD9 Tetraspanin: a new pathway for the regulation of inflammation? *Front Immunol* 2018; **9**: 2316. [Medline] [CrossRef]
3. **Ikeyama S, Koyama M, Yamaoko M, Sasada R, Miyake M.** Suppression of cell motility and metastasis by transfection with human motility-related protein (MRP-1/CD9) DNA. *J Exp Med* 1993; **177**: 1231–1237. [Medline] [CrossRef]
4. **Miyake M, Koyama M, Seno M, Ikeyama S.** Identification of the motility-related protein (MRP-1), recognized by monoclonal antibody M31-15, which inhibits cell motility. *J Exp Med* 1991; **174**: 1347–1354. [Medline] [CrossRef]
5. **Wang HX, Li Q, Sharma C, Knoblich K, Hemler ME.** Tetraspanin protein contributions to cancer. *Biochem Soc Trans* 2011; **39**: 547–552. [Medline] [CrossRef]
6. **Jin Y, Takeda Y, Kondo Y, Tripathi LP, Kang S, Takeshita H, Kuhara H, Maeda Y, Higashiguchi M, Miyake K, Morimura O, Koba T, Hayama Y, Koyama S, Nakanishi K, Iwasaki T, Tetsumoto S, Tsujino K, Kuroyama M, Iwahori K, Hirata H, Takimoto T, Suzuki M, Nagatomo I, Sugimoto K, Fujii Y, Kida H, Mizuguchi K, Ito M, Kijima T, Rakugi H, Mekada E, Tachibana I, Kumanogoh A.** Double deletion of tetraspanins CD9 and CD81 in mice leads to a syndrome resembling accelerated aging. *Sci Rep* 2018; **8**: 5145. [Medline] [CrossRef]
7. **Miyake M, Nakano K, Ieki Y, Adachi M, Huang CL, Itoi S, Koh T, Taki T.** Motility related protein 1 (MRP-1/CD9) expression: inverse correlation with metastases in breast cancer. *Cancer Res* 1995; **55**: 4127–4131. [Medline]
8. **Horiguchi K, Nakakura T, Yoshida S, Tsukada T, Kanno N, Hasegawa R, Takigami S, Ohsako S, Kato T, Kato Y.** Identification of THY1 as a novel thyrotrope marker and THY1 antibody-mediated thyrotrope isolation in the rat anterior pituitary gland. *Biochem Biophys Res Commun* 2016; **480**: 273–279. [Medline] [CrossRef]
9. **Yoshida S, Fujiwara K, Nishihara H, Kato T, Yashiro T, Kato Y.** Retinoic acid signalling is a candidate regulator of the expression of pituitary-specific transcription factor Prop1 in the developing rodent pituitary. *J Neuroendocrinol* 2018; **30**: e12570. [Medline] [CrossRef]
10. **Horiguchi K, Fujiwara K, Yoshida S, Nakakura T, Arae K, Tsukada T, Hasegawa R, Takigami S, Ohsako S, Yashiro T, Kato T, Kato Y.** Isolation and characterisation of CD9-positive pituitary adult stem/progenitor cells in rats. *Sci Rep* 2018; **8**: 5533. [Medline] [CrossRef]
11. **Blumenthal A, Giebel J, Ummanni R, Schlüter R, Endlich K, Endlich N.** Morphology and migration of podocytes are affected by CD151 levels. *Am J Physiol Renal Physiol* 2012; **302**: F1265–F1277. [Medline] [CrossRef]
12. **Naulé L, Picot M, Martini M, Parmentier C, Hardin-Pouzet H, Keller M, Franceschini I, Mhaouty-Kodja S.** Neuroendocrine and behavioral effects of maternal exposure to oral bisphenol A in female mice. *J Endocrinol* 2014; **220**: 375–388. [Medline] [CrossRef]
13. **Zhang P, Ge Z, Wang H, Feng W, Sun X, Chu X, Jiang C, Wang Y, Zhu D, Bi Y.** Prolactin improves hepatic steatosis via CD36 pathway. *J Hepatol* 2018; **68**: 1247–1255. [Medline] [CrossRef]
14. **Zou X, Kwon SH, Jiang K, Ferguson CM, Puranik AS, Zhu X, Lerman LO.** Renal scattered tubular-like cells confer protective effects in the stenotic murine kidney mediated by release of extracellular vesicles. *Sci Rep* 2018; **8**: 1263. [Medline] [CrossRef]
15. **Boucheix C, Rubinstein E.** Tetraspanins. *Cell Mol Life Sci* 2001; **58**: 1189–1205. [Medline] [CrossRef]
16. **Hemler ME.** Tetraspanin functions and associated microdomains. *Nat Rev Mol Cell Biol* 2005; **6**: 801–811. [Medline] [CrossRef]
17. **Borellini F, Oka T.** Growth control and differentiation in mammary epithelial cells. *Environ Health Perspect* 1989; **80**: 85–99. [Medline] [CrossRef]
18. **Haslam SZ, Levely ML.** Estrogen responsiveness of normal mouse mammary cells in primary cell culture: association of mammary fibroblasts with estrogenic regulation of progesterone receptors. *Endocrinology* 1985; **116**: 1835–1844. [Medline] [CrossRef]
19. **Arendt LM, Kuperwasser C.** Form and function: how estrogen and progesterone regulate the mammary epithelial hierarchy. *J Mammary Gland Biol Neoplasia* 2015; **20**: 9–25. [Medline] [CrossRef]
20. **Brisken C, O'Malley B.** Hormone action in the mammary gland. *Cold Spring Harb Perspect Biol* 2010; **2**: a003178. [Medline] [CrossRef]
21. **Hennighausen L, Westphal C, Sankaran L, Pittius CW.** Regulation of expression of genes for milk proteins. *Biotechnology* 1991; **16**: 65–74. [Medline]
22. **O'Leary KA, Shea MP, Salituro S, Blohm CE, Schuler LA.** Prolactin alters the mammary epithelial hierarchy, increasing progenitors and facilitating ovarian steroid action. *Stem Cell Reports* 2017; **9**: 1167–1179. [Medline] [CrossRef]
23. **Berditchevski F.** Complexes of tetraspanins with integrins: more than meets the eye. *J Cell Sci* 2001; **114**: 4143–4151. [Medline]
24. **Kotha J, Longhurst C, Appling W, Jennings LK.** Tetraspanin CD9 regulates beta 1 integrin activation and enhances cell motility to fibronectin via a PI-3 kinase-dependent pathway. *Exp Cell Res* 2008; **314**: 1811–1822. [Medline] [CrossRef]
25. **Streuli CH, Edwards GM.** Control of normal mammary epithelial phenotype by integrins. *J Mammary Gland Biol Neoplasia* 1998; **3**: 151–163. [Medline] [CrossRef]
26. **Romagnoli M, Bresson L, Di-Cicco A, Pérez-Lanzón M, Legoix P, Baulande S, de la Grange P, De Arcangelis A, Georges-Labouesse E, Sonnenberg A, Deugnier MA, Glukhova MA, Faraldo MM.** Laminin-binding integrins are essential for the maintenance of functional mammary secretory epithelium in lactation. *Development* 2020; **147**: 147. [Medline] [CrossRef]
27. **Zöller M.** Tetraspanins: push and pull in suppressing and promoting metastasis. *Nat Rev Cancer* 2009; **9**: 40–55. [Medline] [CrossRef]
28. **Nishida-Aoki N, Tominaga N, Takeshita F, Sonoda H, Yoshioka Y, Ochiya T.** Disruption of circulating extracellular vesicles as a novel therapeutic strategy against cancer metastasis. *Mol Ther* 2017; **25**: 181–191. [Medline] [CrossRef]
29. **Vaswani K, Mitchell MD, Holland OJ, Qin Koh Y, Hill RJ, Harb T, Davies PSW, Peiris H.** A method for the isolation of exosomes from human and bovine milk. *J Nutr Metab* 2019; **2019**: 5764740. [Medline] [CrossRef]
30. **Hendrix A, Hume AN.** Exosome signaling in mammary gland development and cancer. *Int J Dev Biol* 2011; **55**: 879–887. [Medline] [CrossRef]